ANISOTROPIC EFFECTS AND MASTER CURVES FOR RUBBERS WITH sp^2 CARBON ALLOTROPES: TOWARDS LIGHT WEIGHT MATERIALS

Galimberti Maurizio,[a]

Guerra Silvia,[a] Infortuna Giuseppe,[a] Barbera Vincenzina,[a] Bernardi Andrea,[a] Mastinu Gianpiero,[a] Agnelli Silvia,[b] Pandini Stefano,[b]

[a]Politecnico di Milano, Department of Chemistry, Materials and Chemical Engineering "G. Natta", Via Mancinelli 7, 20131 Milano, Italy

[b] Università degli Studi di Brescia, Dipartimento di Ingegneria Meccanica e Industriale, Via Branze 38, 25123 Brescia, Italy

Presented at the Fall 192nd Technical Meeting
of the Rubber Division of the American Chemical Society, Inc.
Cleveland (OH)
October 9 - 12, 2017

ABSTRACT

This work presents the preparation of lightweight rubber materials with nanosized sp^2 carbon allotropes and discusses the anisotropic nonlinear mechanical behavior of composites based on these nanofillers.

Composites were prepared with either poly(styrene-co-butadiene) or poly(1,4-cis-isoprene) as the polymer matrix and either carbon black (CB) or carbon nanotubes (CNT) or hybrid CB/CNT as the filler systems. The initial modulus of the composite ($G'_{\gamma min}$) was determined through dynamic mechanical shear tests and was correlated with the specific interfacial area (i.a.), calculated through the product of filler surface area, density and volume fraction. Common correlation was established, the equation of the common interpolating curve was derived and was used to design composites with the same modulus and lower density, substituting part of CB with lower amount of the carbon allotrope with larger surface area, CNT.

Anisotropic nonlinear mechanical behavior was found for nanocomposites based on CNT and poly(1,4-cis-isoprene), prepared by melt blending, calendering and compression molding. An orthotropic and transversally isotropic response was observed: dynamic-mechanical moduli were very similar inside the sheet plane and very different from those in the orthogonal direction. Hence, energy dissipation is not isotropic in CNT filled rubber composites. Such mechanical behavior was correlated with the material structure: alternate areas containing large or low CNT amount and preferential orientation of CNT were observed. In spite of this anisotropic behavior, the validity of the above mentioned mastercurve was confirmed.

INTRODUCTION

sp^2 carbon allotropes are known as efficient reinforcing fillers for rubber materials. Carbon black (CB) [1] was used already in the early 1900's and, over the last decades, nanofillers such as carbon nanotubes (CNT), both single [2-3] and multi-walled [4-5], graphene (G) [6-9] or graphitic nanofillers made by few layers of graphene [10-13] have been playing a role of increasing importance. CB is made by primary nanometric particles, fused together to form micron-size aggregates: it is a so called nanostructured filler. Nanofillers bring individual nanometric particles into the polymer matrix. The great interest on nanofillers is due to their large surface area and hence to the large interfacial area they are able to establish with the polymer matrix. Nanofillers such as GRM and CNT have anisometric nature. Nanoplatelets and nanofibers achieve the largest values of interfacial area and can exhibit preferential orientation inside a matrix, leading to anisotropic properties.

In this manuscript, the reinforcing ability of CB and CNT in different rubber matrices was studied, with the aim to identify common features and behaviour of nano and nanostructured sp^2 carbon allotropes and to elucidate the role played by fillers' anisometry.

The correlation between the mechanical reinforcement and the filler-polymer interfacial area (i.a.) was investigated. The filler-polymer interfacial area (i.a.) is the surface made available by the filler per unit volume of composite and was calculated through Equation 1, as the product

$$i.a. = s.a. * \rho * \phi \quad (1)$$

where s.a. is the surface area, ρ is the filler density and ϕ is the filler volume fraction. The research performed by some of the authors revealed the correlation between i.a. and both dynamic modulus [14] and vulcanization parameters such as induction time and activation energy [15] for composites based on either CB or CNT or on the hybrid filler system and poly(isoprene) rubber. In the present work, composites were prepared, via melt blending, with either CB or CNT as the

carbon allotropes, as the only filler or as CB/CNT hybrid filler system, and with either poly(1,4-cis-isoprene) (IR) or poly(styrene-co-butadiene) (SBR) as the rubber matrices. Peroxide crosslinking was performed. Dynamic moduli were determined through dynamic-mechanical measurements in the torsion mode: strain sweep experiments were performed up to 25% as strain amplitude and the modulus at minimum strain $G'_{\gamma min}$ and $\Delta G'$ difference ($G'_{\gamma min}$ - $G'_{25\%}$) were determined.

Composites based on natural rubber (NR), poly(1,4-cis-isoprene) from *Hevea Brasiliensis*, and either CB or CNT as the carbon fillers, were used to study the material anisotropy. Melt blending of NR was performed with various amounts of either CB or CNT, both in the absence and in the presence of continuous filler network, and calendering, compression molding and peroxide curing were performed. Dynamic-mechanical measurements were done in the plane of the plate and also in perpendicular direction. The nonlinear mechanical behavior of the crosslinked composites was studied through the shear dynamic mechanical response at various strains. First results have been already reported elsewhere [16].

EXPERIMENTAL SECTION

Materials

Rubber samples

Synthetic poly(1,4-*cis*-isoprene) (PI) was SKI3 (Nizhnekamskneftechim Export), with 70 Mooney Units (MU) as Mooney viscosity (M_L(1+4)100°C).

Synthetic poly(styrene-co-butadiene) (SBR) was Nipol NS 522 (Zeon Corporation), with 39 mass% of bound styrene, 37.5 mass% of extension oil and 62 Mooney Units (MU) as Mooney viscosity (ML(1+4)100°C).

Poly(1,4-cis-isoprene) from *Hevea Brasiliensis* (natural rubber, NR) was SMR GP, with 65 Mooney Units as Mooney viscosity (ML(1+4)100°C), from Lee Rubber.

Carbon Fillers

Carbon Black N326 (CB) was from Cabot, with 30 nm as mean diameter of spherical primary particles and surface area of 77 m^2/g.

Two types of Multiwall Carbon Nanotubes (CNT) were used. NANOCYL® NC7000™ (CNT(N)), with carbon purity of 90%, average length of about 1.5 μm and surface area of 275 m^2/g. Baytubes® C150 P (CNT(B)) from Bayer Material Science, with a chemical purity higher than 95 wt%, a length in the 1–10 μm range and surface area of 200 m^2/g.

Filler density was: $\rho_{CB} = \rho_{CNT} = 1.8$ g/cm^3.

Surface area was determined through BET.

Compounds' ingredients

Dicumyl peroxide (DCUP) (Arkema Inc).

Study of the effect of interfacial area on dynamic-mechanical properties

Composition of rubber (nano)composites

For the study of the effects of filler interfacial area on the mechanical properties, both SBR and IR were used as elastomers. Composites were all prepared with 100 phr of elastomer and 1.4 phr DCUP. The composites were filled with various amounts of CB, or of CNT(B) in IR, or CNT(N) in SBR. Furthermore, also hybrid filler composites were prepared by the addition of both CNT and CB to the same matrix. The filler amount of the composites is reported in **Table I** for IR and **Table II** for SBR.

TABLE I

TABLE II

Preparation

Composites were prepared via melt blending in a Brabender® type internal mixer having 50 mL mixing room. All the samples were prepared with the same procedure, reported as follows. 50 g of the polymer were fed to the mixer and masticated for 1 min at 80 °C with rotors rotating at 60 rpm. Filler was added, mixing was performed for 4 min and the composite was finally discharged at about 90 °C as the temperature. The composite reached room temperature and was fed again to the mixer at a temperature of about 50°C. Peroxide was added, mixing was performed for 3 minutes with rotors rotating at 60 rpm, composite was discharged and was homogenized by passing them 5 times through a two roll mill operating at 50 °C, with the front roll rotating at 30 rpm and the back roll rotating at 38 rpm and 1 cm as the nip between the rolls.

Dynamic-mechanical characterization

Dynamic-mechanical measurements in the torsion mode were carried out with a Monsanto R.P.A. 2000 rheometer. A first strain sweep (0.1–25% strain amplitude) was performed at 50°C on un-cross-linked samples, to cancel their thermo-mechanical history. The samples were then kept in the instrument at the minimum strain amplitude (0.1%) for 10 min to achieve fully equilibrated conditions. A strain sweep (0.1–25% strain amplitude) was then performed with a frequency of 1 Hz. Curing was carried out at 150°C with a frequency of 1.67 Hz and an angle of 6.98%. Curing time was 30 min. On cross-linked samples, a first strain sweep (0.1–25% strain amplitude) was performed at 50°C, then the sample was kept in the instrument at the minimum strain amplitude (0.1%) for 10 min, to achieve fully equilibrated conditions. Finally, a strain sweep (0.1–25% strain amplitude) was performed with a frequency of 1 Hz.

Study of the effect of anisometry on dynamic-mechanical properties

Composition of rubber (nano)composites

For the investigation of anisotropic properties, composites were based on 100 phr HNR and 1.4 phr DCUP. Composites were based either on CB, or on CNT(B). The content of CB was 35 phr. Various amounts of CNT(B) were used: 0, 4, 15 and 35 phr.

Preparation

Composites were prepared as reported above, by using NR in place of IR and SBR.

Dynamic-mechanical characterization

Samples for the measurement of mechanical anisotropy were vulcanized in the form of square sheets with a thickness of 3 mm, by a compression molding machine, operating for 10 min at 170°C with 3.5 MPa pressure. The samples were previously mixed in a Brabender® type internal mixer, with 50 mL mixing chamber, then further homogenized by passing them through a two roll mill operating at 50°C. Mechanics tests were carried out on rectangular specimens cut from the rubber sheets (nominal dimensions: height = 6 mm, width = thickness = 3 mm). Dynamic mechanical tests were carried out on the cured rectangular specimens in shear mode by a dynamic-mechanical analyzer Q800 (TA Instruments). After mechanical conditioning, a strain sweep (0.02–30% strain amplitude) was performed with a frequency of 1 Hz, at room temperature.

Two main test configurations were used, which are schematically represented in **Figure 1**. In the "in plane" (IP) configuration, shear strains could be applied in the plane of the sheet, and in the "through-thickness" (TT) configuration, shear strains were applied perpendicularly to the main plane of the sheet. In both configurations, shear strains were applied either along direction 1 or perpendicularly, i.e. along direction 2, as in the example of **Figure 1**. **Figure 1** shows also a schematic representation of the structuring of CNT within the rubber plate, as should be expected

from the production process of the rubber plate: random orientation in the main sheet plane, and layered structure across the sheet thickness.

FIGURE 1

RESULTS AND DISCUSSION SECTION

Study of the effect of interfacial area on dynamic-mechanical properties

Composites were studied with either IR or SBR as the polymer matrix and either CNT or CB as the sp^2 carbon allotropes. Recipes are shown in in **Table I** and in **Table II**. In the case of composites based on IR, composites with the same total volume % were compared: CNT and CB were used as the only filler or were used in equal amount in hybrid filler systems. Investigation on this type of composites has been already performed [14]. Experiments have been reproduced in the present work and further composites have been prepared, in particular with higher CB content. Composites based on SBR were prepared with a given content of CB (5, 10 and 15 as volume %), adding various amounts of CNT.

Dynamic-mechanical properties were determined by performing strain sweep experiments. Storage shear modulus G' at the minimum shear strain amplitude $G'_{\gamma min}$, (γ_{min} = 0.1% strain), and $\Delta G'$ difference ($G'_{\gamma min} - G'_{25\%}$) were determined.

In **Figure 2**, the dependence on total filler volume % of $G'_{\gamma min}$ (**Figure 2a**) and $\Delta G'$ (**Figure 2b**), for composites based on IR, is shown.

FIGURE 2

For the same total filler volume %, both $G'_{\gamma min}$ and $\Delta G'$ are remarkably higher for CNT based composites: the highest values are for the composites with CNT as the only filler.

In **Figure 3**, the dependence on total filler volume % of $G'_{\gamma min}$ (**Figure 3a)** and $\Delta G'$ (**Figure 3b**), for composites based on SBR, is shown.

FIGURE 3

Analogously to what observed in the case of IR based composites, CNT leads to higher values of both $G'_{\gamma min}$ and $\Delta G'$ and the highest values are with CNT as the only filler.

It is well known that CNT leads to large mechanical reinforcement of polymer melts and elastomers and also to large non-linearity of the composite dynamic modulus [17, 18]. Besides considerations on cost and impact on health and environment, the remarkable improvement of mechanical properties would make CNT ideal candidates for partial (or even complete!) replacement of carbon black in rubber compounds. However, the large Payne Effect [19] brought about by CNT is one of main stumbling blocks which prevents the large-scale CNT application, whatever is the Payne effect mechanism, thixotropy above the filler percolation threshold [20-23] or polymer-filler bonding and debonding [24-32].

$G'_{\gamma min}$, and $\Delta G'$ ($G'_{\gamma min}$ - $G'_{25\%}$) were then correlated with the specific interfacial area, calculated according to Equation 1. As reported in the introduction, the interfacial area is the surface made available by the filler per volume unit of composite. Indeed, in the text below, measure unit of interfacial area is m^2/cm^3, to indicate the square meters potentially available on the filler per volume unit of composite. The interfacial area of hybrid filler systems was calculated as the sum of the i.a. of each filler, by applying Equation 2:

$$\text{i.a.} = A_{i\,CB} * \rho_{CB} * \phi_{CB} + A_{i\,CNT} * \rho_{CNT} * \phi_{CNT} \qquad (2)$$

Values of $G'_{\gamma min}$ for composites of Table I and Table II were normalized with respect to $G'_{\gamma min}$ of the matrix and were plotted as a function of the interfacial area, calculated by applying Equation 1 and Equation 2. Graphs in **Figure 4** show the dependence of $(G'/G'_m)_{\gamma min}$ on the interfacial area for all the composites of **Table I** and **Table II**, based on either IR or SBR, on either CB or CNT or

CB/CNT. Graph in **Figure 4a** shows correlation for all the points, whereas graph in **Figure 4b** shows a magnification in the 0-25 (m^2/cm^3) interval of the interfacial area.

FIGURE 4

In the graph of **Figure 4b**, a common line, a sort of "master curve" appears able to fit all the points. It is worth observing that such interval of interfacial area corresponds to CB and CNT content of about 45 and 11.5 parts per hundred parts of polymer, which are indeed relevant contents for these fillers. Scattering observed in **Figure 4a** could be due to different reasons. Points due to only CNT lie below the line and this could be due to difficult mixing of the nanofiller. Points due to composites based on SBR, in particular with the hybrid filler system, lie above the line. It is reported in the literature that an aromatic polymer, such as SBR [33], and carbon black [34-37] help the dispersion of CNT. It is worth adding that synergistic effects on mechanical reinforcement have been reported for hybrid filler systems formed by CNT and CB [38, 39-40, 41-45].

Graph in **Figure 5** shows the dependence of $\Delta G'$ ($G'_{\gamma min}$ - $G'_{25\%}$) on the specific interfacial area.

FIGURE 5

It is indeed worth observing that a common line, again a sort of "master curve", is able to fit all the points, with very minor scattering up to a pretty large value of interfacial area. This graph leads to a very important conclusion: large Payne effect is not necessarily correlated with CNT. All the sp^2 carbon allotropes give the same value of dynamic modulus and the same modulus non-linearity, if they bring the same interfacial area into the composite.

To describe the curve of **Figure 4b**, the following equation, Equation 3, was derived:

$$G'_{\gamma min}/G'_{m} = e^{0.043 i.a.} \quad (3)$$

Design of lightweight materials

The approach followed to design lightweight materials is summarized in **Figure 6**.

FIGURE 6

Target of the research activity was the dynamic rigidity of a rubber composite. Such rigidity could be obtained with an appropriate combination of sp^2 carbon allotropes. The pathway followed to design the lightweight material is shown in **Figure 7.**

FIGURE 7

Starting point is the equation of the master curve of **Figure 4b**, Equation 3. Upon defining the target value of the dynamic modulus, the value of interfacial area of Equation 2 can be obtained by knowing the density and the volume fraction of each carbon filler. For given values of filler volume fractions, the density of the composite (ρ_C) is given by the Equation 4, based on the rule of mixtures, under the assumption that the rubber based is made only by the rubber and the fillers:

$$\rho_C = \rho_{CB} * \phi_{CB} + \rho_{CNT} * \phi_{CNT} + \rho_m * (1- \phi_{CB} - \phi_{CNT}) \quad (4)$$

$G'_{\gamma min}$ interfacial area values of Equation 4 could be obtained by using different amounts of CNT and CB, as single fillers or in hybrid filler systems.

Composite density was plotted as a function of $\phi_{CNT}/(\phi_{CB}+\phi_{CNT})$ for composites with $G'_{\gamma min}$ modulus in the range from 0.43 to 1.56 MPa. Curves obtained are shown in the graph in **Figure 8**. Lighter composites are obtained with larger amount of CNT. The ratio between CNT amount and total filler amount, defined as $\phi_{CNT}/(\phi_{CB}+\phi_{CNT})$, ranges from 0, for composites based only on CB, to 1 for composites based only on CNT.

FIGURE 8

Study of the mechanical anisotropy of dynamic-mechanical properties

The mechanical anisotropy of HNR systems filled with CB or CNT(B) was investigated by measuring the dynamic moduli along different directions of specimens cut from rubber sheets, as explained in the experimental part. For each material studied, moduli were measured in shear mode, in two different configurations: IP, when the strain was applied in the plane of the rubber sheet, and TT, when the strain was through the thickness (see **Figure 1**). **Figure 9** shows two representative curves, G' vs shear strain amplitude, for each material studied. Black curves are measured in IP and grey curves in TT configuration.

FIGURE 9

Dynamic moduli of CNT filled nanocomposites in **Figure 9a** show a strong dependence on the direction of strain. Generally speaking, the materials are stiffer when the strains are applied in the plane of the sheet rather than through the thickness. By contrast, no significant differences are found when testing the shear properties in plane along different directions (namely 1 or 2 in **Figure 1**). The results are typical of the behavior of a transversal isotropic material. This behavior could be interpreted as a consequence of a random orientation of the filler particles in the sheet plane, and of their planar piling up through the sheet thickness. Evidence of preferential CNT orientation was confirmed and quantitatively observed also by coupling bright field Transmission Electron Microscopy and Selected Area Electron Diffraction [16].

Anisotropic effects appear to be caused by the presence of the filler. In fact, HNR was found to be essentially isotropic. The filler aspect ratio has a relevant effect on the material anisotropy. In fact,

only a slight anisotropic behaviour is observed with 35 phr CB, a filler with relatively low aspect ratio.

The difference between IP and TT results depends thus on filler type and amount. In order to compare different systems, an anisotropy index is here defined as the value measured in IP over the value measured in TT configuration. The initial modulus (i.e. at 0.025% strain amplitude, $G'_{0.025\%}$) is the value in the moduli curves mostly influenced by the filler structure. The anisotropy index of $G'_{0.025\%}$ is 1.03±0.02 for HNR and only 1.10±0.02 with 35 phr CB. Such value is practically 1 if compared to those obtained with CNT: 1.88±0.04 (with 4 phr CNT), 2.25±0.04 (with 15 phr CNT), 1.95±0.06 (with 35 phr CNT). It is clear therefore that CNT are able to promote a remarkable level of anisotropy already at small contents. By increasing the filler content, anisotropy tends to increase up to 15 phr CNT and then slightly decreases: this result is possibly due to the higher difficulty in orientation of the bundles of CNT at such high contents.

Conclusions

This work presents a quantitative correlation between the surface area made available by a sp^2 carbon allotrope in a rubber composite and the initial storage modulus of the composite. This correlation appears to be independent of the type of the rubber matrix.

Composites were prepared based on either poly(styrene-co-butadiene) or poly(1,4-cis-isoprene) as the polymer matrix, with either carbon nanotubes or carbon black or hybrid carbon filler systems. Composites initial modulus were measured with dynamic-mechanical measurements in the shear mode and were correlated with the interfacial area, obtaining a common curve, a sort of master curve, up to a CB and CNT content of about 30 and 10 as mass%.

sp^2 carbon allotropes with larger surface area, such as the nanosized carbon nanotubes, lead to larger composite modulus than nanostructured carbon allotropes, such as carbon black, which have low surface area. Nanosized sp^2 carbon allotropes such as CNT appear thus the ideal candidate for the preparation of lightweight materials.

Nanocomposites were prepared, based on natural rubber, with different CNT content: 4, 15, 35 phr and experienced calendering and compression molding. Dynamic mechanical response of peroxide crosslinked samples was investigated, at various strain levels, in different directions, defined as "in-plane" and "through-thickness". Typical dynamic-mechanical behavior of a transversally isotropic material was observed. "in-plane" moduli were remarkably different from "through-thickness" moduli, revealing the anisotropy of nanocomposites. The "through-thickness" moduli measured along different strain directions in the sheet had very similar values, indicating a transversally isotropic material. A remarkable anisotropic nonlinear mechanical behavior of CNT based nanocomposites is shown. Anisotropy was also observed for $\Delta G'$. Hence, this work shows that energy dissipation is not an isotropic phenomenon in polymer nanocomposites based on CNT.

REFERENCES

[1] Donnet J. B., Custodero E., *The Science and Technology of Rubber Third Ed.*, **2005**, Elsevier Academic Press, Chapter 8, 367.

[2] Iijima S., Ichihashi T., *Nature,* **1993**; 363-603.

[3] Bethune D.S., Kiang C.H., de Vries M.S., Gorman G., Savoy R., Vazquez J. et al., *Nature,* **1993**, 363-605

[4] Iijima S., *Nature,* **1991**, 354-356.

[5] Monthioux M., Kuznetsov V.L., *Carbon*, **2006**; 44(9), 1621-1623.

[6] Novoselov K. S., Geim A. K., Morozov S. V., Jiang D., Zhang Y., Dubonos S. V., Grigorieva I. V., Firsov A. A., *Science,* **2004**, 306, 666–669.

[7] Geim A. K. and Novoselov K. S., *Nat. Mater.*, **2007**, 6(3), 183–191.

[8] Allen M. J., Tung V. C. and Kaner R. B., *Chem. Rev.*, **2010**, 110, 132–145.

[9] Zhu Y. W. et al., *Adv. Mater.*, **2010**, 22, 3906–3924.

[10] Geng Y., Wang S. J. and Kim J.-K., *J. Colloid Interface Sci.*, **2009**, 336(2), 592–598.

[11] Kavan L., Yum J. H. and Gratzel M., *ACS Nano,* **2011**, 5, 165–172.

[12] Nieto A., Lahiri D. and Agarwal A., *Carbon*, **2012**, 50(11), 4068–4070.

[13] Paton K. R., Varrla E., Backes C., Smith R. J., Khan U., O'Neill A., Boland C., Lotya M., Istrate O. M., King P., Higgins T., Barwich S., May P., Puczkarski P., Ahmed I., Moebius M., Pettersson H., Long E., Coelho J., O'Brien S. E., McGuire E. K., Mendoza Sanchez B., Duesberg G. S., McEvoy N., Pennycook T. J., *Nat. Mater.*, **2014**, 13, 624–630.

[14] Agnelli S., Cipolletti V., Musto S., Coombs M., Conzatti L., Pandini S., Riccò T., Galimberti M., *eXPRESS Polymer Letters*, **2014**, 8(6), 436.

[15] Musto S., Barbera V., Cipolletti V., Citterio A., Galimberti M., *eXPRESS Polymer Letters*, **2017**, 11(6), 435–448.

[16] Agnelli S., Pandini S., Serafini A., Musto S., Galimberti M., *Macromolecules*, **2016**, 49(22), 8686–8696.

[17] Bokobza L., *Polymer* **2007**, 48, 4907–4920.

[18] Galimberti M., Coombs M., Riccio P., Riccò T., Passera S., Pandini S., Conzatti L., Ravasio A., Tritto I., *Macromol. Mater. Eng.*, **2012,** 298, 241-251.

[19] Payne A. R., Whittaker R. E., *Rubber Chemistry and Technology*, **1971**, 44, 440–478.

[20] Robertson C.G., Roland C.M., *Rubber Chemistry and Technology*, **2008**, 81(3), 506-522.

[21] Bohm G.A., Tomaszewski W., Cole W., Hogan T., *Polymer* **2010**, 51, 2057-2068.

[22] Heinrich G. and Kluppel M., *Filled Elastomers Drug Delivery Systems*, **2002**, Volume 160 of the series Advances in Polymer Science, pp 1-44.

[23] Maier P.G., Goritz D., *Kautschuk Gummi Kunststoffe*, **1996**, 49(1), 18-21.

[24] Maier P.G., D. Goritz, *Kautschuk Gummi Kunststoffe* **1996,** 49(1), 18-21.

[25] Chazeau L., Brown J.D., Yanyo L.C., Sternstein S.S., *Polymer composites* **2000**, 21(2), 202-222.

[26] Sternstein S. S., Ai-Jun Zhu. *Macromolecules*, **2002**, 35(19), 7262-7273.

[27] Montes H., Lequeux F., Berriot J., *Macromolecules*, **2003**, 36(21), 8107-8118.

[28] Zhu Z., Thompson T., Wang S. Q., von Meerwall E. D., Halasa A., *Macromolecules*, **2005**, 38(21), 8816-8824.

[29] Kalfus J., Jancar J., *Polymer Composites* **2007**, 365-371.

[30] Jancar J., Douglas J.F., Starr F. W., Kumar S. K., Cassagnau P., Lesser A. J., Buehler M. J., *Polymer* **2010**, 51, 3321-3343.

[31] Funt J.M., *Rubber chemistry and technology*, **1988**, 61(5), 842-865.

[32] Gauthier C., Reynaud E., Vassoille R., and Ladouce-Stelandre L., *Polymer* **2004**, 45(8), 2761-2771.

[33] Tsuchiya K., Sakai A., Nagaoka T., Uchida K., Futukawa T., Yajima H., *Composites Science and Technology* **2011**, 71(8), 1098-1104.

[34] Yunkong P., Kueseng P., Wirasate S., Huynh C., Rattanasom N., *Polymer Testing* **2015**, 41, 172-183.

[35] Thaptong P., Sirisinha C., Thepsuwan U., Sae-Oui P., *Polymer-Plastics Technology and Engineering* **2014**, 53(8), 818-823.

[36] Bokobza L., *Vibrational Spectroscopy*, **2009**, 51(1), 52-59.

[37] Rahmani M., Belin C., Bruneel J.L., El Bounia N.E., *Journal of Polymer Science Part B: Polymer Physics*, **2008**, 46(18), 1939-1951.

[38] Galimberti M., Cipolletti V., Musto S., Cioppa S., Peli G., Mauro M., Guerra G., Agnelli S., Riccò T., Kumar V., *Rubber Chemistry And Technology*, **2014**, 87(3), 417-442.

[39] Galimberti M., Agnelli S., Cipolletti V., *Progress in Rubber Nanocomposites*, *1st Edition*, Woodhead Publishing, **2017**.

[40] Agnelli S., Cipolletti V., Musto S., Coombs M., Conzatti L., Pandini S., Riccò T., Galimberti M., *eXPRESS Polymer Letters*, **2014**, 8, 436.

[41] Szeluga U., Kumanek B., Trzebicka B., *Composites Part A: Applied Science and Manufacturing*, **2015**, 73, 204-231.

[42] Galimberti M., Coombs M., Riccio P., Riccò T., Passera S., Pandini S., Conzatti L., Ravasio A., Tritto I., *Macromolecular Materials and Engineering*, **2013**, 298(2), 241-251.

[43] Dong B., Liu C., Lu Y., Wu Y., *Journal of Applied Polymer Science*, **2015**, 132(25), 42075.

[44] Galimberti M., Coombs M., Cipolletti V., Riccò T., Agnelli S., Pandini S., *Kautschuk Gummi Kunstoffe*, **2013**, 7, 31–36.

[45] Bhowmick A.K., Bhattacharya M., Mitra S., Journal of Elastomers and Plastics, **2010**, (42), 517.

FIGURE 1

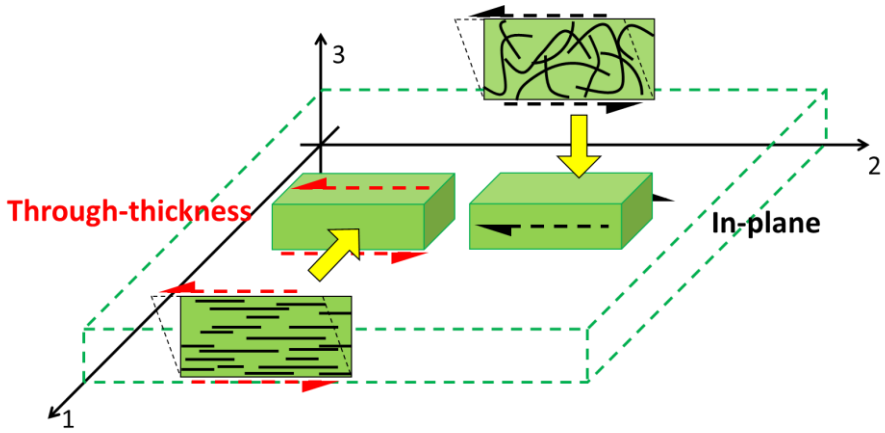

FIGURE 2

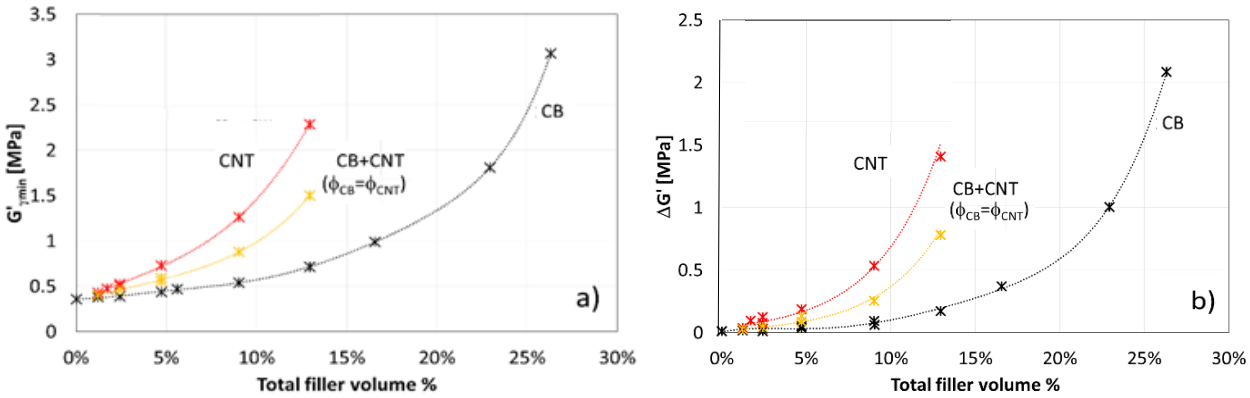
3.5
3
2.5
2
1.5
1
0.5
0
G'ymin [MPa]
CNT
CB+CNT
(ϕCB=ϕCNT)
CB
a)
0%
5%
10%
15%
20%
25%
30%
Total filler volume %
2.5
2
1.5
1
0.5
0
ΔG' [MPa]
CNT
CB+CNT
(ϕCB=ϕCNT)
CB
b)
0%
5%
10%
15%
20%
25%
30%
Total filler volume %

FIGURE 3

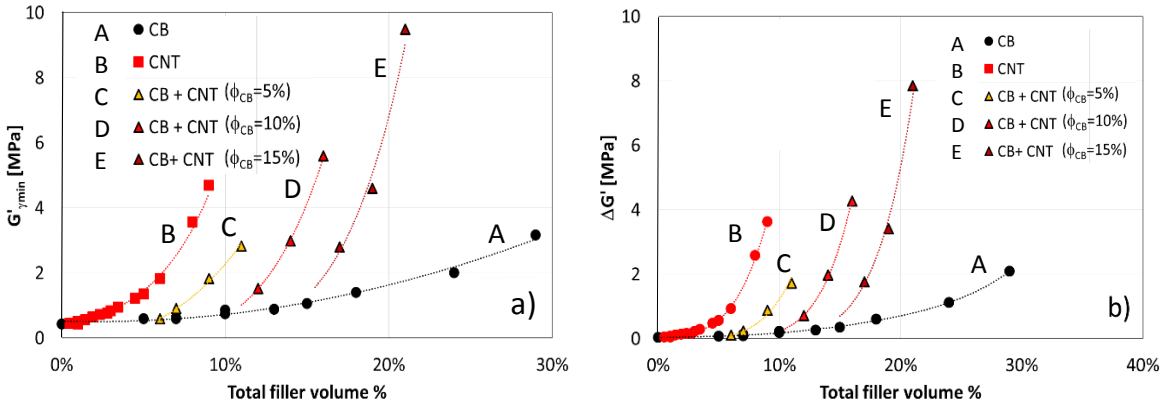
A CB
B CNT
C CB + CNT (ϕ_{CB}=5%)
D CB + CNT (ϕ_{CB}=10%)
E CB+ CNT (ϕ_{CB}=15%)
G'$_{\gamma min}$ [MPa]
Total filler volume %
a)
ΔG' [MPa]
Total filler volume %
b)

FIGURE 4

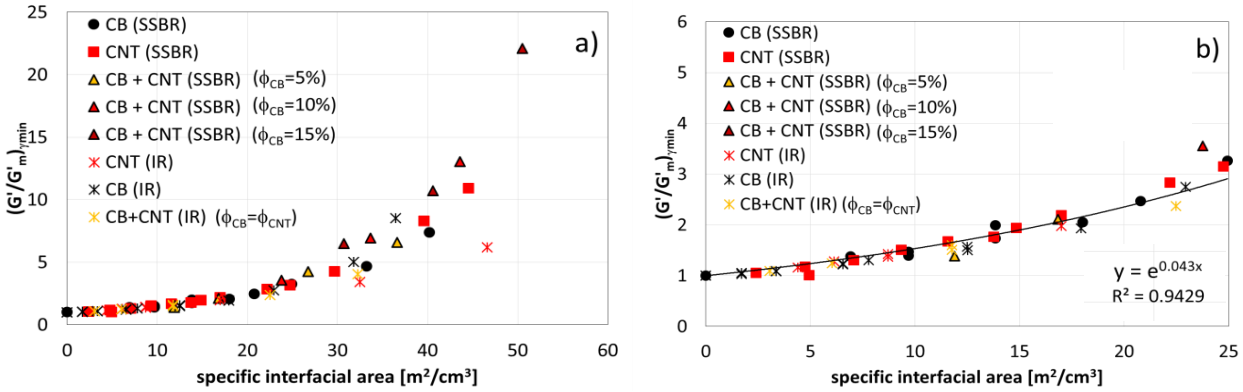
a)
CB (SSBR)
CNT (SSBR)
CB + CNT (SSBR) (ϕCB=5%)
CB + CNT (SSBR) (ϕCB=10%)
CB + CNT (SSBR) (ϕCB=15%)
CNT (IR)
CB (IR)
CB+CNT (IR) (ϕCB=ϕCNT)
(G'/G'm)γmin
specific interfacial area [m²/cm³]
b)
y = e0.043x
R² = 0.9429

FIGURE 5

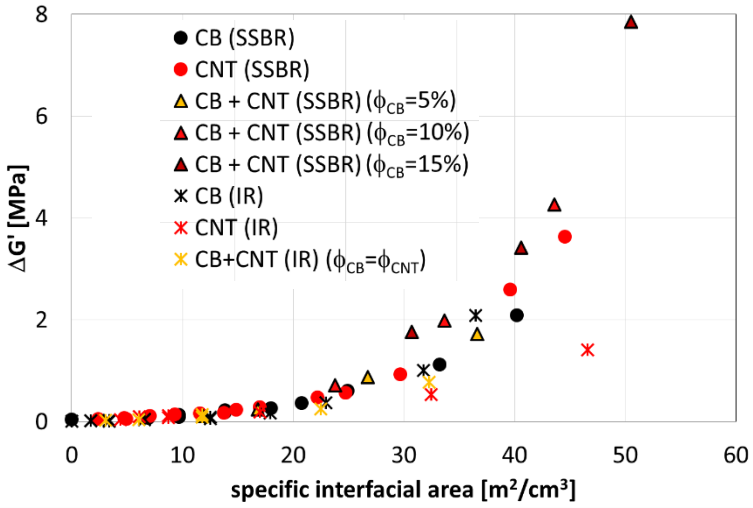
CB (SSBR)
CNT (SSBR)
CB + CNT (SSBR) (ϕCB=5%)
CB + CNT (SSBR) (ϕCB=10%)
CB + CNT (SSBR) (ϕCB=15%)
CB (IR)
CNT (IR)
CB+CNT (IR) (ϕCB=ϕCNT)
ΔG' [MPa]
specific interfacial area [m²/cm³]
0
2
4
6
8
0
10
20
30
40
50
60

FIGURE 6

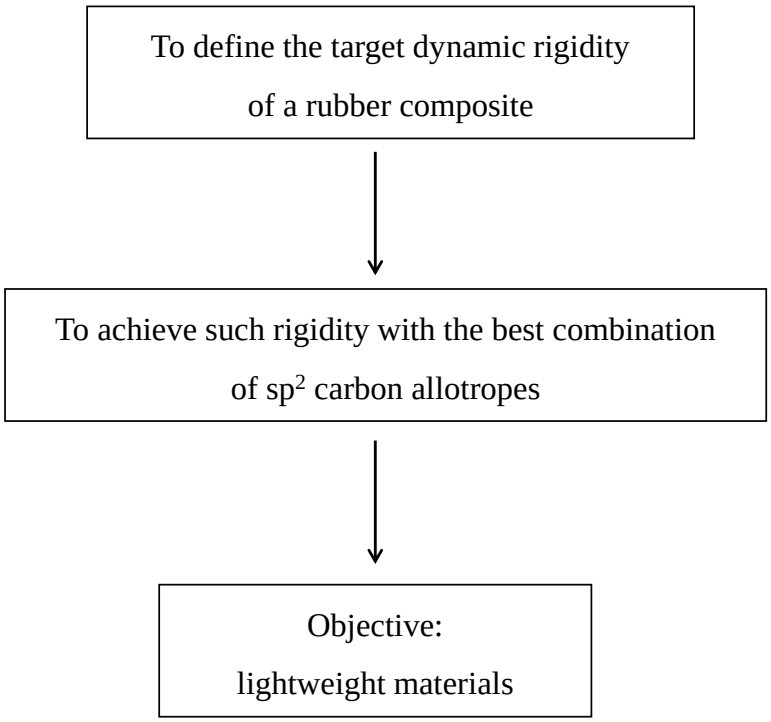
To define the target dynamic rigidity
of a rubber composite
To achieve such rigidity with the best combination
of sp2 carbon allotropes
Objective:
lightweight materials

FIGURE 7

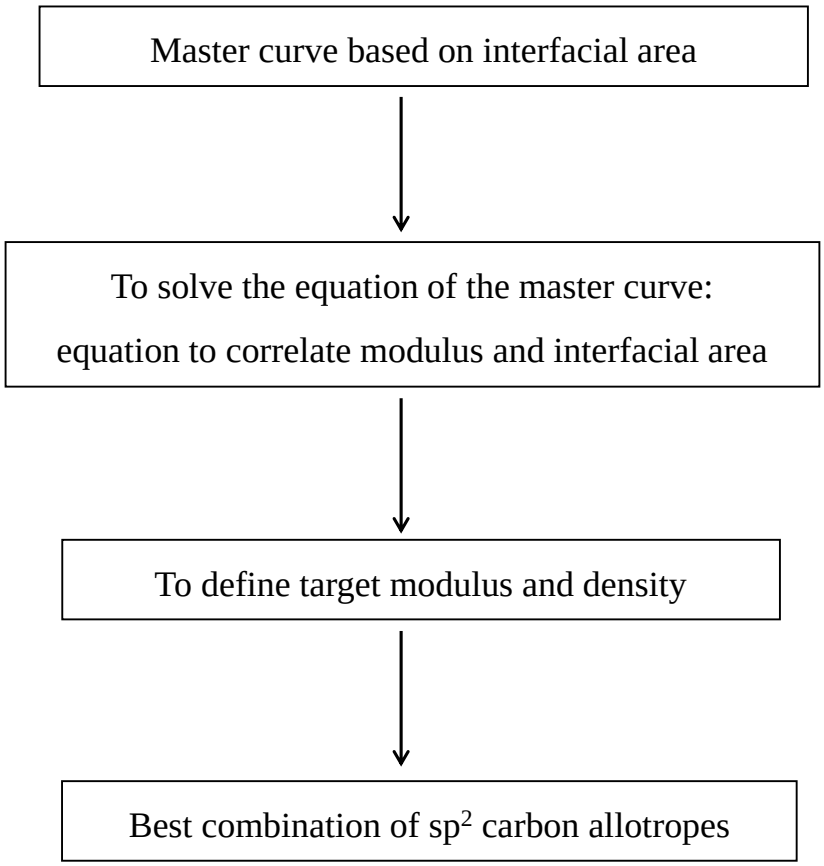
Master curve based on interfacial area
To solve the equation of the master curve:
equation to correlate modulus and interfacial area
To define target modulus and density
Best combination of sp2 carbon allotropes

FIGURE 8

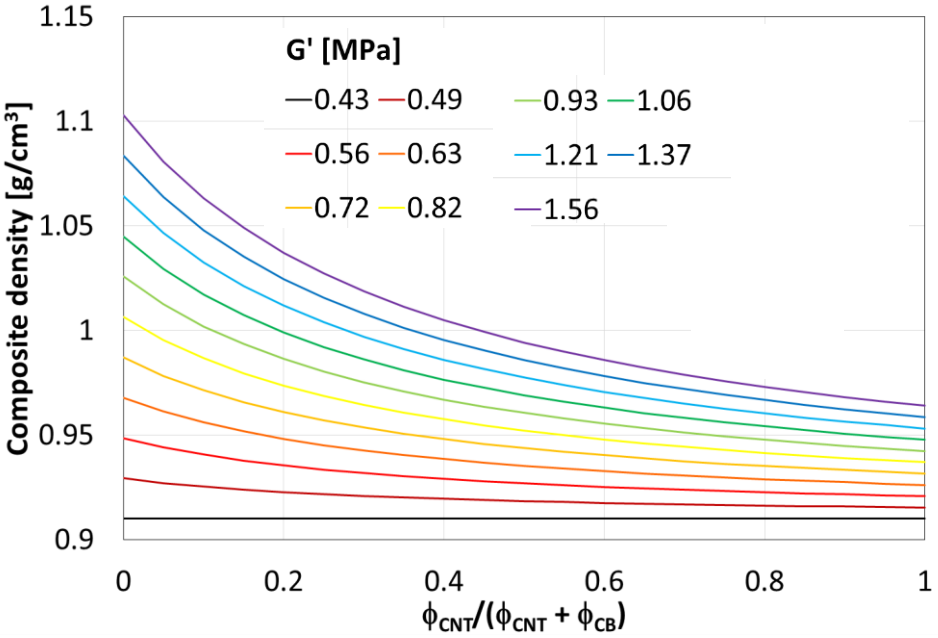
G' [MPa]
0.43
0.49
0.93
1.06
0.56
0.63
1.21
1.37
0.72
0.82
1.56
Composite density [g/cm³]
1.15
1.1
1.05
1
0.95
0.9
0
0.2
0.4
0.6
0.8
1
ϕCNT/(ϕCNT + ϕCB)

FIGURE 9

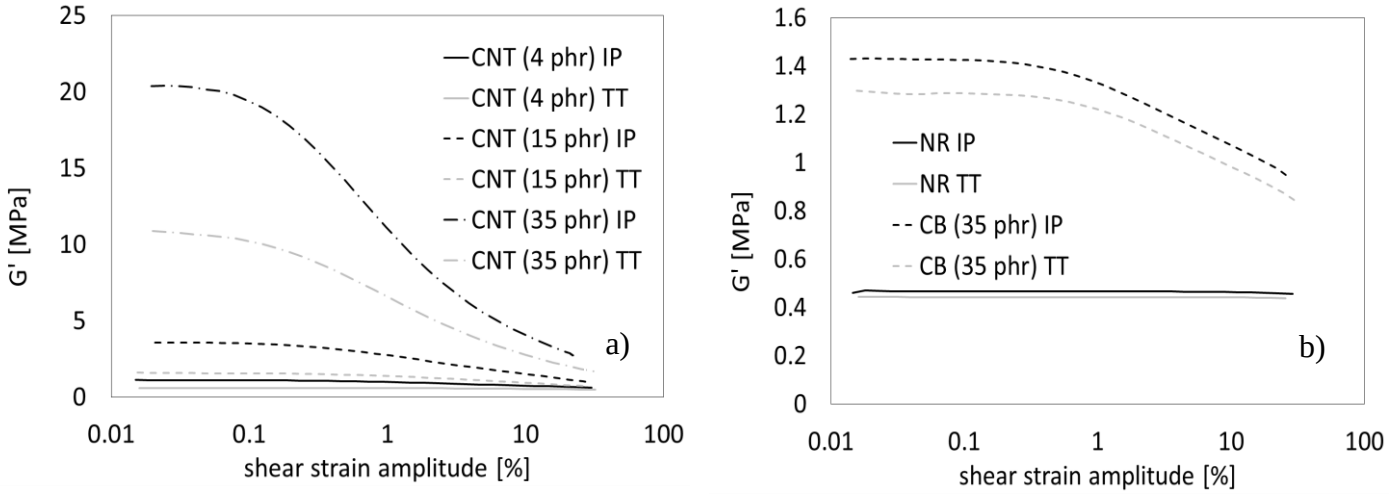
25
20
15
10
5
0
G' [MPa]
0.01
0.1
1
10
100
shear strain amplitude [%]
CNT (4 phr) IP
CNT (4 phr) TT
CNT (15 phr) IP
CNT (15 phr) TT
CNT (35 phr) IP
CNT (35 phr) TT
a)
1.6
1.4
1.2
1
0.8
0.6
0.4
0.2
0
G' [MPa]
0.01
0.1
1
10
100
shear strain amplitude [%]
NR IP
NR TT
CB (35 phr) IP
CB (35 phr) TT
b)

LIST OF FIGURE CAPTIONS

Figure 1. Schematic representation of parallelepiped samples for dynamic-mechanical tests taken from a rubber sheet. Dashed arrows indicate shear strains as applied in TT (left side) and IP (right side) configurations. Expected CNT organization is also shown.

Figure 2. $G'_{\gamma min}$ (a) and $\Delta G'$ ($G'_{\gamma min}$ - $G'_{25\%}$) (b) vs total filler volume % for composites based on IR of Table I.

Figure 3. $G'_{\gamma min}$ (a) and $\Delta G'$ ($G'_{\gamma min}$ - $G'_{25\%}$) (b) vs total filler volume % for composites based on SBR of Table II.

Figure 4. $(G'/G'_m)_{\gamma min}$ vs specific interfacial area for composites of Table 1 and Table 2(a); magnification of the 0 -25 (m^2/cm^3) interval of the interfacial area with exponential fitting curve (b)

Figure 5. $\Delta G'$ ($G'_{\gamma min}$ - $G'_{25\%}$) vs specific interfacial area for composites of Table 1 and Table 2

Figure 6. Pathway for the preparation of lightweight materials from the master curve of mechanical reinforcement (Equation 3)

Figure 7. Pathway for the preparation of lightweight materials from the master curve of mechanical reinforcement (Equation 3)

Figure 8. Composite density vs $\phi_{CNT}/(\phi_{CB}+\phi_{CNT})$ for composites with $G'_{\gamma min}$ modulus in the range from 0.43 to 1.56 MPa.

Figure 9. Representative G' vs shear strain amplitude curves measured both in IP and TT configuration for A) NR filled with 4, 15 and 35 phr CNT(B) and B) neat HNR and HNR + 35 phr CB

TABLE I

RECIPES OF IR BASED COMPOSITES. CONTENTS ARE IN PHR

Single filler compounds							
CNT(B)	0	1.25	2.50	5.00	10.00	15.00	30.00
CB	0	1.25	2.50	5.00	10.00	15.00	30.00
Hybrid filler compounds							
CNT(B)/CB			1.25/1.25	2.50/2.50	5.00/5.00	7.50/7.50	15.00/15.00

TABLE II

RECIPES OF SBR BASED COMPOSITES. CONTENTS ARE IN PHR

Single filler compounds		
CNT(N)	0; 1; 2; 3; 4; 5; 6; 6.5; 7.5; 10; 11; 14; 18; 20	
CB	0; 10; 15; 20; 22; 30; 35; 45; 50; 60	
Hybrid filler compounds		
CB	10	+ CNT(N): 0 ÷ 14
CB	22	+ CNT(N): 0 ÷ 14
CB	35	+ CNT(N): 0 ÷ 14